Model-informed design of antibiotic therapy against antimicrobial resistance

Tandar, S.T.

Section III

Collateral Sensitivity

Chapter 8

Clinical prevalence of collateral sensitivity: a systematic exploration of multi-center antimicrobial surveillance data

Sebastian T. Tandar*
Laura B. Zwep*
Sjoukje H. S. Woudt
Annelot F. Schoffelen
Wiep Klaas Smits
Linda B. S. Aulin
Apostolos Liakopoulos
J. G. Coen van Hasselt
Infectious Diseases Surveillance Information System-Antimicrobial Resistance Study Group

Lancet Microbe (2026), 101274. Advance online publication.

* authors contributed equally to this work.

Abstract

Collateral effects arise when resistance to one antibiotic alters the susceptibility of one bacterial strain to another, resulting in either increased (collateral sensitivity; CS) or decreased (collateral resistance; CR) susceptibility. CS-based antibiotic treatment offers a promising strategy against antibiotic resistance. To date, the clinical occurrence of CS between bacterial strains and species remains to be further evaluated. Our study aims to evaluate the occurrence patterns of CS in clinical settings.

In this study, we analyzed large-scale antimicrobial resistance surveillance data from three datasets, covering over 5 million minimum inhibitory concentration (MIC) measurements across 86 antibiotics and 30 pathogen species, to identify collateral effect interactions. Pairwise and three-way collateral effects were quantified to assess species-wide trends in both CS and CR within individual pathogen species. Additionally, we compared the prevalence of CS between and within antibiotic classes. By comparing CS occurrence across species, we identified CS interactions conserved across several pathogens.

We found a low occurrence of CS in clinical strains, with 364 of 12 024 species-antibiotic pairs (3.0%) affected, compared to 5044 cases (42.0%) of CR. Most CS interactions involved antibiotics from different classes, except for β-lactams, which showed a 41 (34.2%) of 120 occurrences of intraclass CS. We identified six CS pairs that were conserved across four bacterial species, including several highly virulent pathogens belonging to the ESKAPEE group. Three of these conserved CS pairs were associated with a higher MIC towards colistin. Only one three-way CS interaction was shared across four pathogen species. The collateral effect network generated in this study is available via a web application, enabling further data exploration and supporting future research on antibiotic collateral effects.

Several CS interactions were conserved across several clinically relevant pathogens. The identified CS pairs can be considered for the development and application of CS-based antibiotic therapies to prevent and reverse antimicrobial resistance.

Introduction

Antimicrobial resistance (AMR) in bacterial pathogens poses a significant threat to human health[1]. The evolution of AMR can be attributed to multiple underlying cellular mechanisms. AMR mechanisms offer not only a survival strategy against a specific antibiotic, but can also alter the cell's susceptibility to other antibiotics as evolutionary trade-off[2]. The impact of resistance to one antibiotic on susceptibility to another is known as a collateral effect. This effect can appear as decreased susceptibility to another antibiotic, termed collateral resistance (CR), often seen between antibiotics sharing a common resistance mechanism, such as efflux pump overexpression[3]. Resistance to one antibiotic may also lead to increased susceptibility to another antibiotic, which is referred to as collateral sensitivity (CS)[2]. Although the precise mechanisms behind CS often remain elusive, past studies have provided potential mechanistic explanations for its occurrence[2]. For example, *trkH* mutations in *Escherichia coli* were found to mediate resistance to aminoglycosides by reducing proton motive force, hampering aminoglycoside uptake but simultaneously impairing the function of the AcrAB-TolC efflux pump, causing *trkH*-mutant *E. coli* to be more susceptible to other antibiotics[4].

Exploiting the occurrence of CS phenotypes in antibiotic treatment regimens has been suggested as a promising strategy to prevent and reverse AMR[5–7]. The design of a CS-based combination therapy involves selecting and combining drugs such that resistance to one increase susceptibility to the other to overcome antibiotic resistance[2,6–8]. Choosing an effective CS antibiotic pair therefore requires information on the reciprocity and magnitude of the observed collateral effect[8]. Despite the promising potential of CS-based therapies, questions remain about their occurrence and applicability in clinical settings[2], largely because most CS studies have been conducted in controlled laboratory environments. While several CS pairs – such as fluoroquinolone-β-lactam[9] and cefazolin (CZO)-meropenem (MER)[10] – have been identified in clinical *E. coli* isolates, the consistency of CS across different pathogens remains unclear. This consistency is essential to ensure the broader applicability of a particular CS pair for treating a wide range of infections[11]. Therefore, an analysis evaluating the occurrence, magnitude, reciprocity, and consistency of collateral effects across diverse drug pairs and pathogen species is needed.

In the current study we use a pooled, large-scale multicenter antimicrobial surveillance dataset that includes the antibiotic susceptibility profiles of 30 pathogens, including ESKAPEE group pathogens (*Enterococcus faecium*, *Staphylococcus aureus*, *Klebsiella pneumoniae*, *Acinetobacter baumannii*, *Pseudomonas aeruginosa*, Enterobacter *spp.*, and *E. coli*)[12,13]. Using a previously developed statistical inference technique to identify CS[10], we explore the ubiquity of antibiotic pairs demonstrating CS across different species, supporting the potential application of CS-based therapies as a generic treatment in cases where the main pathogen causing the infection is unknown. Additionally, we investigated whether reduced susceptibility to multiple antibiotics better predicts CS to another antibiotic. By investigating the collateral effect network in this dataset, our aim is to advance understanding of the clinical prevalence of CS and to identify CS interactions that may consistently emerge in clinical settings.

Methods

Data source and preprocessing

Clinical isolate minimum inhibitory concentration (MIC) data were acquired and pooled from three datasets, including 1) the National Institutes of Health (The National Institutes of Health (NIH)[14], access date: February 19, 2021), 2) the Infectious Diseases Surveillance Information System – Antimicrobial Resistance (The Dutch National Antimicrobial Resistance Surveillance System (ISIS-AR)[15][15], access date: March 3, 2021), and 3) the Antimicrobial Testing Leadership and Surveillance (Antimicrobial Testing Leadership and Surveillance (ATLAS)[16], access date: November 3, 2023). Each source provided MIC values for multiple pathogens, encompassing a wide range of antibiotic classes. Censored MIC values were imputed as follows: 1) 'less-than-or-equal-to' values were directly used as the imputed MIC, and 2) 'greater-than' values were imputed by doubling the reported value. Rounded MIC values were imputed to the nearest power of 2. MIC obtained from different measurement methods (Fig. S1) were assumed to be equivalent. Data from the NIH database were filtered to exclude non-clinical bacterial isolates. Potentially overlapping entries between datasets were removed based on the reported measurement/strain ID. For each species, the dataset was further curated by excluding antibiotics with fewer than 100 observations, as well as isolates which were only tested for one antibiotic. For the current analysis, entries on *A. baumannii-calcoaceticus* complex were pooled together with that of *A. baumannii*. MIC breakpoint values for each antibiotic-species set were obtained from the 'amr' package[17] in R, using the latest published data from The European Committee on Antimicrobial Susceptibility Testing (EUCAST) or Clinical and Laboratory Standards Institute (CLSI). If the corresponding breakpoint for the exact species was unavailable, the closest available breakpoint value at the next higher taxonomic level was used for analysis.

Pairwise collateral effect quantification

Collateral effect quantification was performed to assess population-wide trends in both CS and CR within specific pathogen species. This analysis was performed using the 'collatRal' package (https://github.com/vanhasseltlab/collatRal)[10]. The pairwise collateral effect quantification involved two drugs denoted as test antibiotic A and focal antibiotic B. Here, a 'focal antibiotic' refers to the primary drug of interest for which resistance characteristics are being examined, while 'test antibiotic' refers to the secondary drug for which potential collateral effect was assessed in relation to resistance to the focal antibiotic. Analysis was performed separately for each species. For each species-antibiotic pair set, MIC data was dichotomized into groups with higher (group $B_{High-MIC}$) and lower (group $B_{Low-MIC}$) MIC towards the focal antibiotic B (**Fig. 1**). The dichotomization threshold (τ) was set at the median MIC for antibiotic B to ensure roughly equal group sizes with a maximum allowed imbalance of 9:1. Collateral effect was quantified as the mean difference of log-MIC value between the groups $B_{High-MIC}$ and $B_{Low-MIC}$ (**Eq. 1**).

$$\phi_{A|B_{\text{High}}} = \overline{\log_2\left(\text{MIC}_{A|B_{\text{High}}}\right)} - \overline{\log_2\left(\text{MIC}_{A|B_{\text{Low}}}\right)} \qquad \textbf{Eq. 1}$$

The identification of collateral effect was determined by hypothesis testing with a null hypothesis of $\phi = 0$. The alternative hypotheses were $\phi < 0$ for CS and $\phi > 0$ for CR. A false discovery rate (FDR)-adjusted *p-value* threshold of 0.05 was used to determine

the statistical significance of the tested collateral effect interaction[10], which was used to ensure the identified collateral effects reflect a relevant change in antibiotic susceptibility (**Fig. 1**). All possible antibiotic pairs were tested bidirectionally. The prevalence of CS interaction between antibiotic classes was evaluated based on the occurrence rate of CS between each pair of antibiotic classes.

In this analysis, collateral effects were assessed solely from antibiotic susceptibility profiles without determining underlying mechanisms. The primary focus of this analysis is to identify "collateral sensitivity", defined as cases where a higher MIC for the focal antibiotic corresponds to a lower MIC for the test antibiotic. Conversely, the term "collateral resistance" is used to describe cases where a higher MIC for the focal antibiotic is associated with a higher MIC for the test antibiotic without distinguishing "collateral resistance" from "co-resistance". Thus, the term "collateral resistance" was used in this study as a general term for both events.

Quantification of three-way CS effects

The current analysis aims to quantify collateral effects involving an antibiotic triplet. For each set of test antibiotic A and focal antibiotics B and C, the strains were grouped into strains with a higher MIC to both B and C ($B_{High}\&C_{High}$) and strains with a lower MIC to either B or C ($B_{Low}|C_{Low}$). Three-way collateral effect of B and C resistance to A (ψ) was quantified by the mean difference of log-MIC value between groups $B_{High}\&C_{High}$ and $B_{Low}|C_{Low}$ (**Eq. 2**). A minimum absolute three-way collateral effect size $|\psi|$ of 0.5 was used to identify physiologically relevant effects.

$$\psi_{A|(B_{\mathrm{High}}\&C_{\mathrm{High}})} = \overline{\log_2\left(\mathrm{MIC}_{A|(B_{\mathrm{High}}\&C_{\mathrm{High}})}\right)} - \overline{\log_2\left(\mathrm{MIC}_{A|(B_{\mathrm{Low}}|C_{\mathrm{Low}})}\right)} \qquad \textbf{Eq. 2}$$

Software

Data (pre-)processing, analysis, and visualization were conducted in R (version 4.3.2). Standardization of antibiotic name, abbreviation, and classification was performed using the AMR package in R[17] (Table. S1).

Role of the funding source

The role of the funder of this study is limited to data collection. The funder was not involved in data analysis, interpretation, or writing of the report.

Results

The analysis was performed on a MIC dataset from 5.10 million isolates pooled from the NIH (0.04%; 2050 isolates), ISIS-AR (88.7%; 4.5 million isolates), and ATLAS (11.2%; 0.6 million isolates) datasets. The ISIS-AR dataset provides extensive information for six ESKAPEE pathogens (Fig. S2A). The NIH and ATLAS databases were incorporated to increase the diversity of antibiotic compounds and pathogen species included in the analysis. The pooled dataset included MIC measurements for 86 antibiotics from human isolates measured in 30 pathogenic species (**Fig. 2A-C** at Appendix p.2; Table S1 at Appendix p.11-12), from 73 countries across multiple continents with most entries originating from the Americas and Europe (Fig. S2C at Appendix p.2). The dataset was not equally distributed across all species and antibiotics. Species with the highest

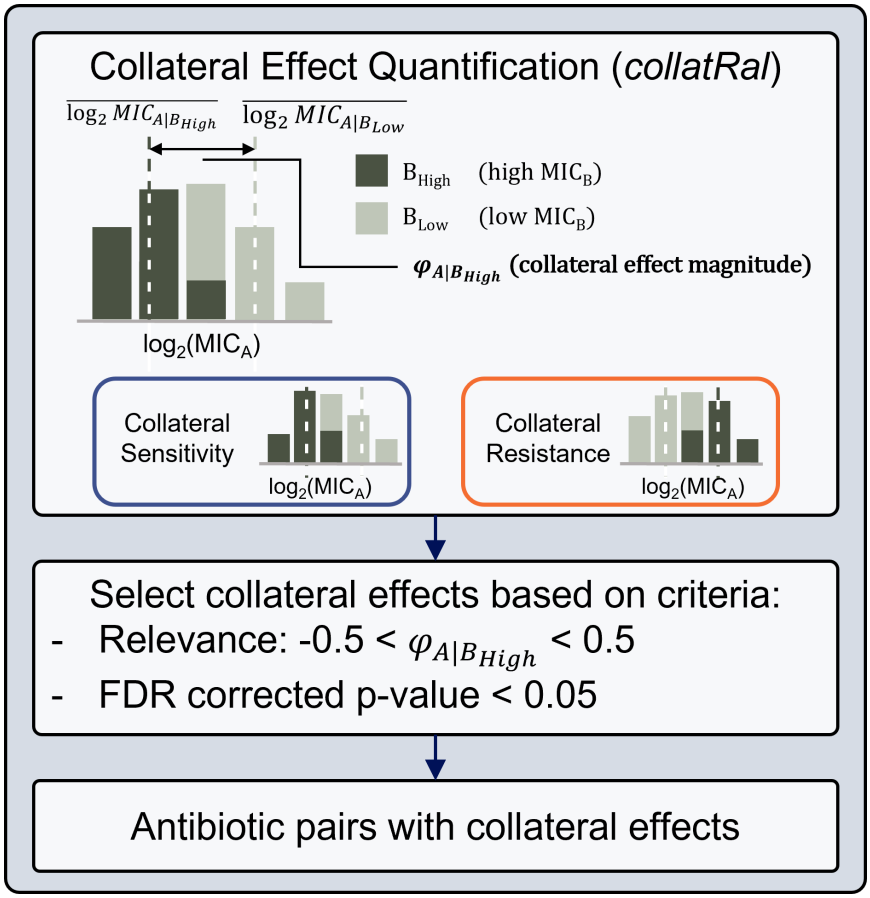

Fig. 1 | Collateral effect quantification workflow. Collateral effect quantification was performed separately for each species and antibiotic pair (test antibiotic A and focal antibiotic B). In this figure, the top panel shows a sample MIC distribution towards test antibiotic A between strains that have a high or low MIC towards the focal antibiotic B. This dichotomization into high or low MIC for the focal antibiotic was based on the median MIC observed for that antibiotic within the tested species. Collateral effect magnitude ϕ was calculated as log2 ratio of the mean MIC value towards antibiotic A observed in groups with a higher MIC (lower susceptibility) and a lower MIC (higher susceptibility) to the focal antibiotic B. Relevant collateral effect pairs were selected based on the magnitude of the collateral effect (ϕ) and statistical significance of the observed MIC difference (FDR-corrected *p-value*).

number of MIC measurements (n) and different antibiotics (d) were *E. coli* (n=2.82×10^6, d=58), *S. aureus* (n=1.05×10^6, d=51), *K. pneumoniae* (n=4.97×10^5, d=53), *P. aeruginosa* (n=4.63×10^5, d=44), and *Streptococcus pneumoniae* (n=6.61×10^4, d=45), which altogether accounted for 4.89×10^6 (95.42%) isolates in the pooled dataset. The combined dataset included a total of 3,630 antibiotic pairs (r), which when stratified by species resulted in 12,024 species-antibiotic pairs.

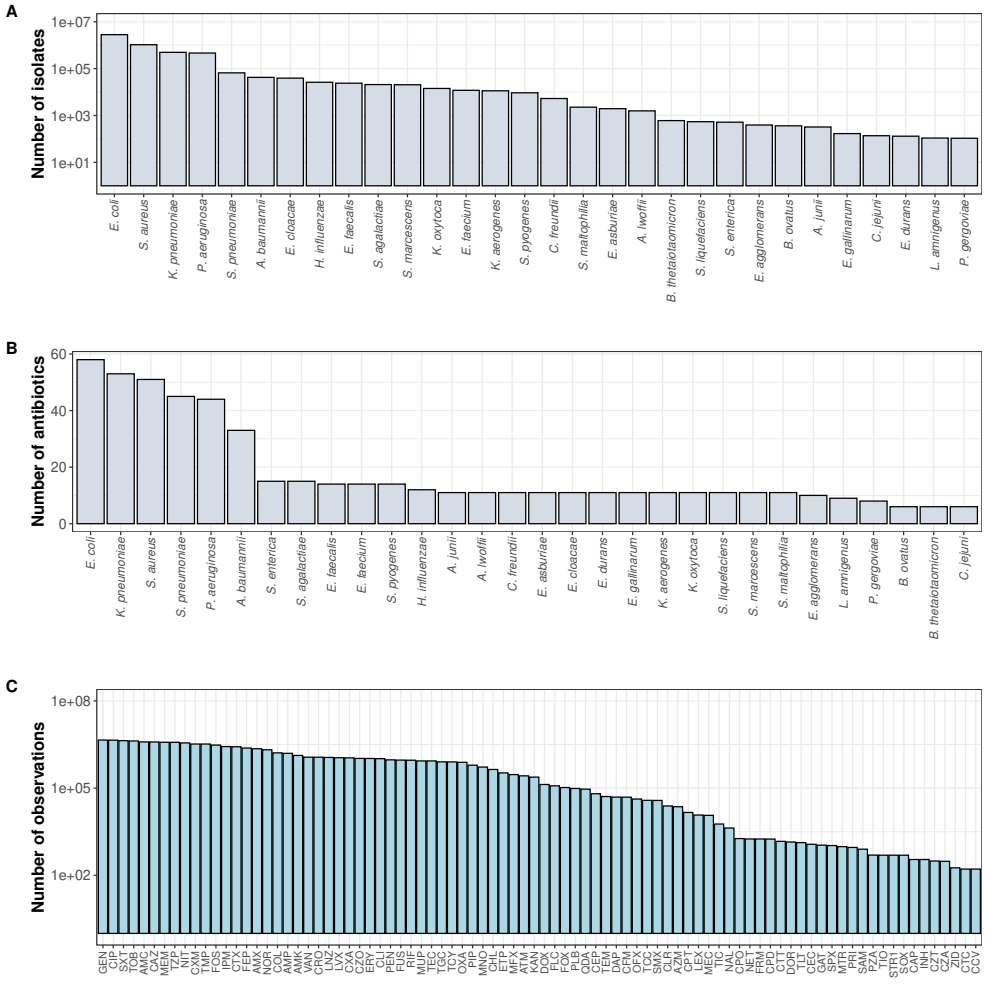

Fig. 2 | Characteristics of the pooled antimicrobial resistance surveillance data. Data was pooled from NIH, ISIS-AR, and ATLAS datasets. A) Number of isolates (observation sets) for each species included in the dataset. Each isolate may be associated with multiple MIC measurements for different antibiotics. B) Number of antibiotics tested on each species included in the dataset. C) Number of MIC measurements identified for each antibiotic included in the dataset. Antibiotics name abbreviations are listed in Table S1.

We identified collateral effects in 5,408 out of the 12,024 (45.0%) tested species-antibiotic pairs. Despite the general prevalence of collateral effects (**Fig. 3A-B**), CS was found to be significantly less prominent than CR (5,044/12,024; **Fig. 3B**), occurring

in 364/12,024 (3.03%) of the observed species-antibiotic pairs (**Fig. 3 B-C**). This aligns with previous reports which also found CS to be less frequent than CR[10,18]. Some CS interactions are specific to either Gram-positive or Gram-negative bacteria, which may reflect the use of certain antibiotics according to Gram-staining classification (Fig. S3).

High MICs to colistin (COL) and chloramphenicol (chloramphenicol (CHL)) showed the highest frequency of relevant CS hits (**Fig. 3**C). Among pairs with CS effects for these antibiotics, reciprocal CS was found in 6 out of 182 (3.3%) pairs for COL and 3 out of 218 (1.4%) pairs for CHL (Table. S2). Inverse proportionality between the MICs of the focal and test antibiotics within a CS pair was not associated with collateral effect magnitude and occurred mainly among pairs with reciprocal CS (Fig. S4).

Collateral effect networks evaluated in this study are accessible through a web application at https://collateralviz.lacdr.leidenuniv.nl. This application enables both general and species/antibiotic-specific explorations of collateral effects through interactive visualization tools. An example exploration of the specific CS network for Haemophilus influenzae is shown in Fig. S5 (Appendix p.5).

While a cutoff collateral effect size $|\phi|$ of 0.5 was applied to select for CS with more relevant impact on test antibiotics MIC, 43.0% of all identified CS was associated with a 2-fold reduction of test antibiotics MIC (equivalent to $\phi \leq -1.0$; Fig. S6A). 14.2% of the identified CS interactions with known MIC breakpoint value for the corresponding species was associated with a decrease in MIC value that recategorized the mean population from above to below the corresponding MIC breakpoint for susceptible isolates (Figs. S6B and S7).

The current analysis evaluated the prevalence of interclass (between antibiotic classes) and intraclass (within antibiotic classes) CS among the identified collateral effect network by comparing the pooled occurrence rates of CS within and between antibiotic classes. The analysis showed that interclass CS interactions were generally more common compared to intraclass CS, with exception of the β-lactam group. Within this group, intraclass CS accounted for up to 34.2% (41 out of 120) of the identified CS interactions (**Fig. 4**). Further division of the β-lactam group into penicillin, cephalosporin, and carbapenem sub-classes revealed that the prevalence of intraclass CS in the β-lactam group was mainly observed within the cephalosporin subclass, in which 21.9% (14 out of 64) of cephalosporin-resistant isolates showed CS to another cephalosporin (Fig. S8). Other intraclass β-lactam CS interactions involving penicillin and carbapenem were associated with increased cephalosporin susceptibility. Antibiotics categorized under 'Other antibacterials' also exhibited intraclass CS, likely due to the integration of multiple smaller antibiotic classes into this group.

To assess the consistency of CS occurrence across different pathogen species, we screened the collateral effect network to identify CS interactions that consistently emerged across multiple species. The majority of detected CS occurrences were found to be unique for one (r=220 pairs) or shared across two (r=45 pairs) species. For example, a strong and reciprocal CS between imipenem (IPM) and CHL was observed in *S. pneumoniae* strains but not in any of the other pathogenic species (Fig. S9). Six antibiotic pairs showed consistent CS across four pathogens (necessarily the same four pathogens). This included (1) azithromycin (AZM) in isolates with a high linezolid (LNZ) MIC, (2) cefuroxime (CXM) in isolates with high MIC to tobramycin (TOB), (3) amoxicillin-clavulanate (AMC) in isolates with high MIC to CHL, as well as (4-6) CZO, ampicillin (AMP), and levofloxacin (LVX) in isolates with high MIC to COL (**Fig. 5A** and **Fig. S9** at Appendix p.9). Notably, all three occurrences of CS in isolates showing a high MIC to COL were conserved across four ESKAPEE pathogens, namely *A. baumannii*,

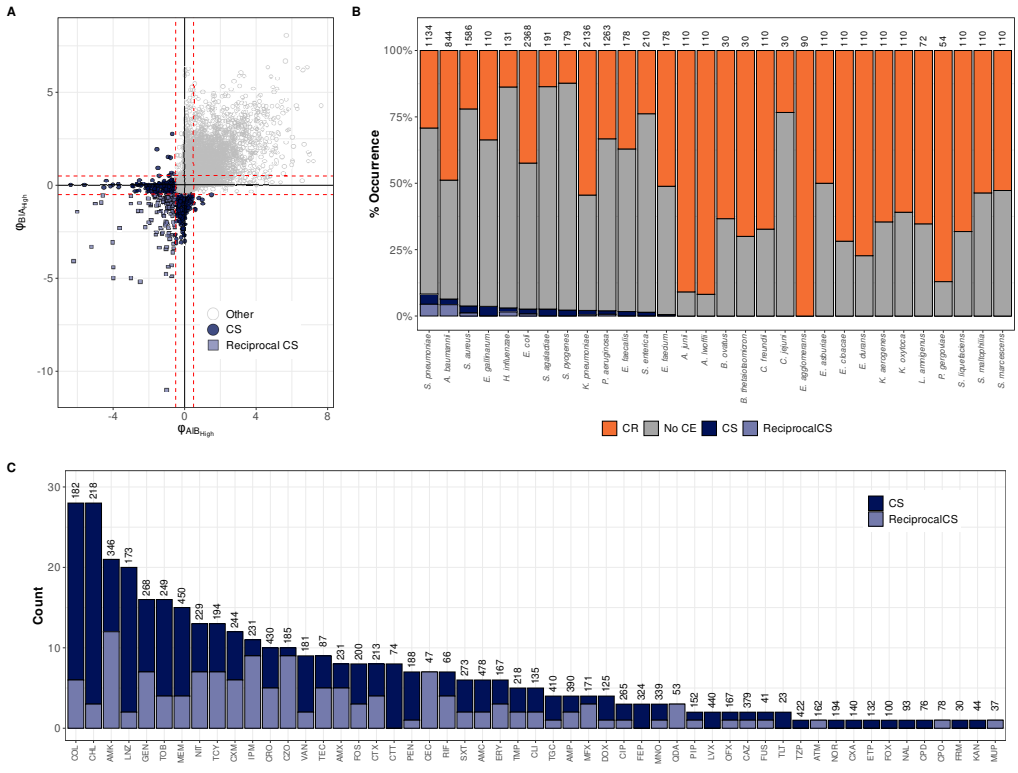

Fig. 3 | Clinical occurrence of collateral effects A) Collateral effect size for each antibiotic pair (using $|\phi| \geq 0.5$ as threshold for relevant collateral effects, denoted by red dashed lines). All tested pairs were categorized based on the direction and reciprocity of the interaction, namely 'reciprocal CS', 'CS', and 'Other' (unidirectional and reciprocal CR as well as no collateral effect). B) Occurrence percentages of CR, CS, reciprocal CS, and no collateral effect (No CE) across different species. The total number of antibiotic pairs tested for each species is shown above the corresponding bars. C) Number of CS pairs identified for each antibiotic. The total number of species-antibiotic pairs tested for the antibiotic of interest (including no collateral effects and CR) were shown above the bars. Antibiotics with no identified CS interaction were excluded. Antibiotics name abbreviations are listed in Table S1.

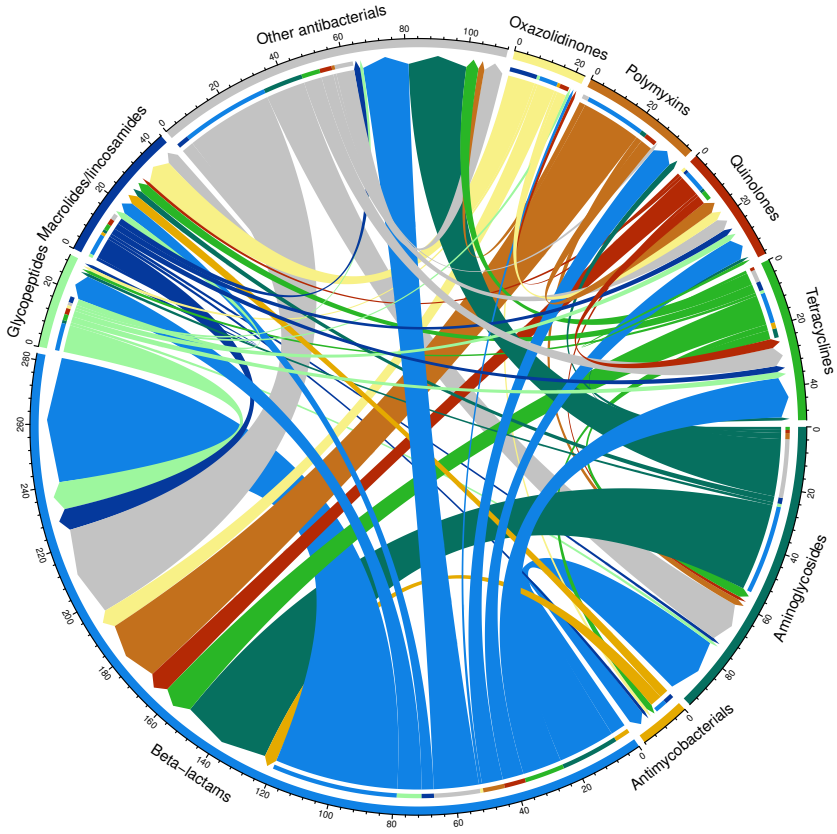

Fig. 4 | Prevalence of interclass and intraclass occurrence of CS. Arrows (chords) originate from the focal antibiotic class and point toward the test antibiotic class. The outer arc colour denotes the antibiotic class at each circle segment, whereas the inner arc colour at the base of each chord denotes the test antibiotic class. Chord width reflects the number of detected CS interactions between focal and test classes. Numbers on the outer arcs indicate the total number of detected CS interactions originating from or received by each antibiotic class. Penicillins, cephalosporins, and carbapenems were grouped as β-lactams; no observed CS involved monobactams. Other antibacterials: chloramphenicol, daptomycin, fosfomycin, fusidic acid, metronidazole, mupirocin, nitrofurantoin, sulfamethoxazole, sulfisoxazole, trimethoprim, trimethoprim and sulfamethoxazole, and zidebactam.

E. coli, *K. pneumoniae*, and *P. aeruginosa*. Among these six pairs, reciprocal CS was observed on COL-CZO pairs in *A. baumannii* and *E. coli* (Fig. S9). This suggests the species-specificity of reciprocal CS. None of the observed CS pairs were shared across more than four species.

Three-way CS evaluation was performed to investigate the potential occurrence of complex CS phenotypes involving antibiotic triplets. The analysis identified 3,186 (4.24% out of 75,056 species-antibiotic triplet sets) three-way CS interactions. For comparison, pairwise CS evaluation covered 3,630 pairs, with 281 (7.74%) pairwise CS interactions identified (**Fig. 5B**). Only one antibiotic triplet showed consistent CS across four species: AZM CS was observed in *Enterococcus faecalis*, *E. faecium*, *Streptococcus agalactiae*, and *S. pneumoniae* isolates with increased MICs to LNZ and MER (Fig. S10).

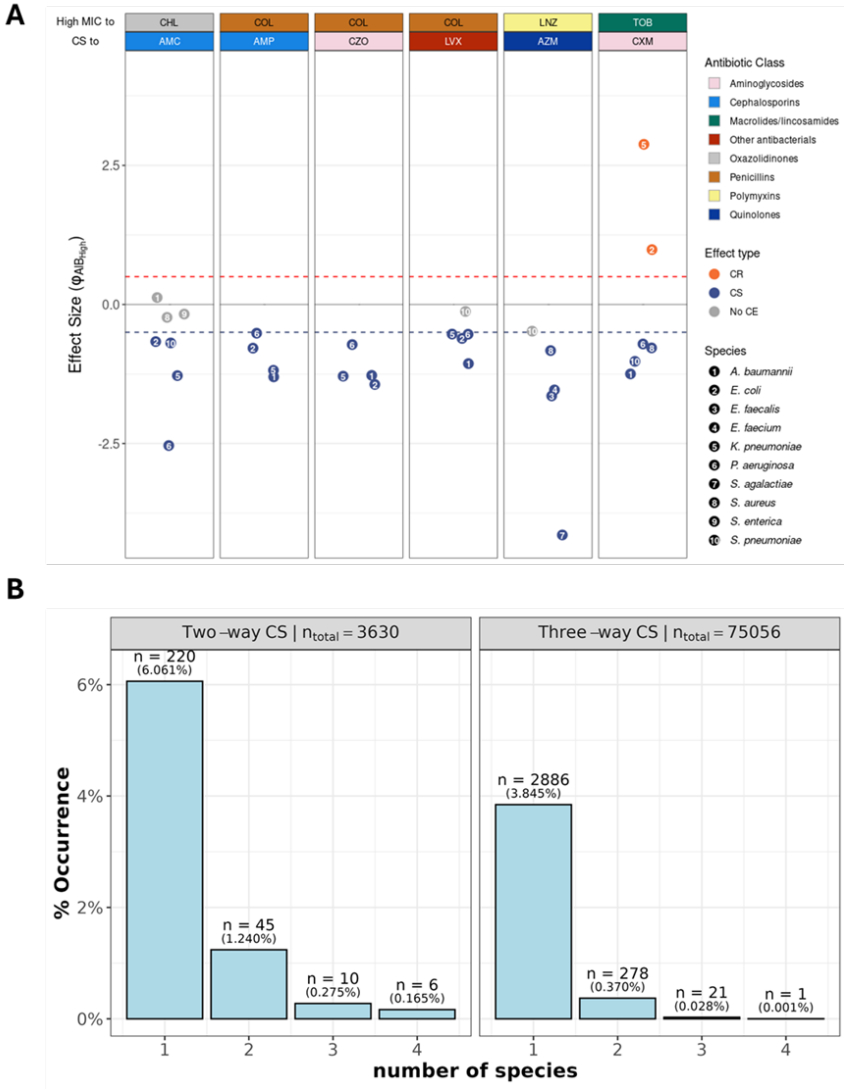

Fig. 5 | Magnitude and bacterial species distribution of consistent CS pairs. A) Consistency of two-antibiotics CS. The CS interactions were considered consistent if the effect was observed in at least 4 different species. A threshold collateral effect size of $|\phi| \geq 0.5$ was applied (dashed red and blue lines). Drug label colors denote the different antibiotic classes between which CS effects were detected. The number of species shown for each antibiotic pair may vary based on data availability, as species with fewer than 100 MIC measurements for a given pair were excluded from the analysis. B) Occurrence rate between consistent two-way and three-way CS across all tested antibiotic pairs and triplets, respectively. The number of antibiotic pairs/triplets is denoted by r. Two-way CS constituted of CS interactions involving two antibiotics, and three-way CS constituted of CS interactions involving three antibiotics. Two- and three-way CS were examined in a total of 3,630 antibiotic pairs and 75,056 antibiotic triplets, respectively. The y-axis represents the occurrence as a percentage of the total number of antibiotic pairs/triplets that showed shared CS across 1, 2, 3, and 4 species. Antibiotic name abbreviations are listed in Table S1.

Discussion

This study aimed to explore the collateral effect network and identify CS antibiotic pairs using a large, multi-center clinical surveillance dataset. While CS is typically assessed by comparing MICs between parental and mutant strains[6,19], such comparisons are challenging in clinical surveillance datasets due to the frequent lack of isolate lineage information. To address this, we focused on species-wide trends. Here, CS was identified from consistent patterns in which a lower MIC to the test antibiotic was associated with a higher MIC to the focal antibiotic across >100 isolates of the same species (**Fig. 1**). Such a pattern indicates an underlying trade-off in antibiotic susceptibility, which by definition constitutes CS. Conversely, if the two MICs varied independently, no statistically significant association would be expected in the aggregate data. By systematically identifying antibiotic pairs with consistent CS, our analysis pinpoints those most likely to produce reproducible CS in clinical settings – a critical consideration for CS-guided therapies[5].

Our analysis does not capture all CS phenotypes within a pathogen species. Instead, it identifies only those that consistently emerge across isolates of each tested species. Thus, our approach may only flag CS phenotypes driven by either a single, highly prevalent resistance mechanism, or by multiple mechanisms that lead to the same phenotype in clinical settings. Consequently, this may limit the current analysis in identifying CS pairs that can be reliably evolved in the lab but are less prevalent in clinical settings, likely due to the more diverse and uncontrolled evolutionary trajectories found in clinical environments[20,21]. For example, aminoglycoside CS consistently emerged in ciprofloxacin (CIP)-resistant *P. aeruginosa* during adaptive laboratory evolution (ALE)[19,22], but this interaction was not detected in our clinical dataset, suggesting it may not be as consistent in real-world settings. ALE studies linked aminoglycoside CS in CIP-resistant strains to mutations in *gyrA/B*, *mexS* (mexEF-oprN), and/or *nfxB* (mexCD-oprJ)[19]. This absence may be due to the presence of alternative CIP resistance mechanisms that do not confer aminoglycoside CS, the occurrence of escape mutations that negate aminoglycoside CS in CIP-resistant strains, or epistatic interactions between the genetic background and specific mutations that resulted in pleiotropic effects. Together, these factors highlight the complexity of translating laboratory CS observations to clinical contexts and help explain the rarity of CS in clinical settings, where environmental conditions drive variable evolutionary trajectories. Seven consistent CS pairs (six pairwise and one three-way CS) were identified. These CS pairs were conserved across four pathogenic species. The rarity of conserved CS, particularly across species, may partly reflect interspecies differences in pathogen physiology and genetic background[12,13,23], which can in turn influence the development of pleiotropic effects, including CS. Given the high prevalence of ESKAPEE pathogens in clinical settings, these consistent CS interactions may offer a strategic advantage in developing CS-based therapies.

Elevated MICs for COL were consistently associated with reduced MICs toward AMP, CZO, and LVX across all Gram-negative pathogens in which these pairs were tested (**Fig. 5A**). Notably, the association between COL resistance and increased susceptibility to other antibiotics has also been highlighted in previous studies[22,24]. One study pinpointed the mechanism of this CS phenotype in COL-resistant Gram-negative bacteria as loss of the lipopolysaccharide layer, which increases membrane permeability and susceptibility to other antibiotics[24]. These findings suggest a shared CS mechanism across COL-resistant Gram-negative pathogens. The alignment between previous

laboratory studies and current clinical observations underscores these CS pairs as both mechanistically characterized and clinically prevalent. Therefore, future studies are encouraged to explore the clinical potential of these CS pairs in combination therapies and to further investigate the occurrence of similar CS phenotypes in other clinically relevant Gram-negative pathogens.

A high number of CS interactions were identified in pathogens showing elevated MIC towards CHL (**Fig. 5C**). This includes three reciprocal CS interactions between CHL and three β-lactam antibiotics, including AMC and IPM in *S. pneumoniae* as well as cefpirome (CPO) in *K. pneumoniae* (Table. S2). This finding is in line with a previous finding of CHL CS in multiple pathogen species[25], and the mechanistically characterized CHL re-sensitization observed in extended spectrum β-lactamase (ESBL)-producing pathogens[26]. Thus, future studies are encouraged to further characterize the underlying mechanisms and pharmacodynamics (PD) CS pairs involving CHL and β-lactams.

Three-way CS interaction was uncommon in this dataset (**Fig. 5B**). The low number of identified interactions may partly reflect the limited measurements available for each antibiotic triplet and the stricter penalties introduced by FDR correction compared with pairwise analyses. One three-way CS, AZM CS in isolates with elevated LNZ and MER MICs, was conserved across four species. While this triplet shows potential as a candidate for three-way CS-based therapy, further investigation is needed to assess its clinical utility.

CS is often assumed to occur primarily between antibiotic pairs from different classes[27]. Consistent with this expectation, our analysis found that CS interactions were predominantly identified between antibiotics of different classes, with the notable exception of β-lactams (**Fig. 4**). Within the β-lactam class, we observed a higher frequency of intraclass CS interactions, particularly among cephalosporins (Fig. S8). The prevalence of intraclass CS within β-lactams may be related to the evolutionary constraints imposed by β-lactamase evolution[28]. Further research is needed to clarify the mechanisms underlying the apparent exclusivity of intraclass CS interactions among β-lactams.

This analysis used pooled MIC data from NIH, ISIS-AR, and ATLAS datasets. The ISIS-AR dataset provides dense information on six ESKAPEE pathogens in the Netherlands, while the NIH and ATLAS databases contribute data on a broader range of species, antibiotics, and geographic regions (Fig. S2A-C). Nevertheless, uneven coverage across antibiotics and pathogens remains in the pooled dataset, limiting our ability to identify CS interactions for underrepresented species and antibiotics. Moreover, the much larger size of the ISIS-AR dataset means that data for certain pathogens are dominated by measurements from the Netherlands, especially for *S. aureus* (89.4%) and *E. coli* (97.2%). As such, the outcomes for these two species may predominantly reflect phenotypes common in Dutch clinics. Future studies incorporating more regionally diverse datasets could further assess the generalizability of the currently identified collateral effect profiles for these two pathogens.

The reliance of the current analysis on MIC values may introduce several limitations. The standard twofold dilution used in MIC assays, combined with the imputation of MIC values required when results are reported as 'greater-than' or 'less-than-or-equal' values, can lead to over- or underestimation of actual antibiotic susceptibility. Consequently, this study may only approximate, and not precisely capture, the magnitude of collateral effects. Nonetheless, MIC remains the most widely available and practical metric for large-scale surveillance and for identifying collateral effects in clinical settings. Subsequent studies aiming to further characterize selected CS pairs identified in the current

analysis may benefit from alternative metrics that offer higher resolution and accuracy in measuring antibiotic susceptibility, such as IC_{50} (concentration to inhibit bacterial growth by 50%) or bactericidal effect EC_{50} (concentration to achieve half-maximal bactericidal effect).

This analysis focused on identifying antibiotic pairs with conserved CS across multiple pathogens. However, the dataset also supports targeted investigations of the collateral effect network. To facilitate this, the collateral effect network evaluated here is available at https://collateralviz.lacdr.leidenuniv.nl for further exploration of pathogen- or antibiotic-specific patterns.

In summary, this large-scale analysis contributes to our understanding of collateral effects by evaluating their occurrence in clinical settings. By highlighting CS interactions conserved across multiple pathogens, our study supports further efforts for developing CS-based therapies that can be effective across a broader range of pathogens. Altogether, these findings support ongoing efforts to translate CS-based strategies into clinical practice to help combat antibiotic resistance.

References

1. Oliphant, C. M., & Eroschenko, K. (2015). Antibiotic Resistance, Part 2: Gram-negative Pathogens. *The Journal for Nurse Practitioners*, *11*(1), 79–86. https://doi.org/10.1016/j.nurpra.2014.10.008
2. Roemhild, R., & Andersson, D. I. (2021). Mechanisms and therapeutic potential of collateral sensitivity to antibiotics. *PLoS Pathogens*, *17*(1), e1009172. https://doi.org/10.1371/journal.ppat.1009172
3. Fernandes, P., Ferreira, B. S., & Cabral, J. M. S. (2003). Solvent tolerance in bacteria: Role of efflux pumps and cross-resistance with antibiotics. *International Journal of Antimicrobial Agents*, *22*(3), 211–216. https://doi.org/10.1016/s0924-8579(03)00209-7
4. Lázár, V., Pal Singh, G., Spohn, R., Nagy, I., Horváth, B., Hrtyan, M., Busa-Fekete, R., Bogos, B., Méhi, O., Csörgő, B., Pósfai, G., Fekete, G., Szappanos, B., Kégl, B., Papp, B., & Pál, C. (2013). Bacterial evolution of antibiotic hypersensitivity. *Molecular Systems Biology*, *9*, 700. https://doi.org/10.1038/msb.2013.57
5. Yekani, M., Azargun, R., Sharifi, S., Nabizadeh, E., Nahand, J. S., Ansari, N. K., Memar, M. Y., & Soki, J. (2023). Collateral sensitivity: An evolutionary trade-off between antibiotic resistance mechanisms, attractive for dealing with drug-resistance crisis. *Health Science Reports*, *6*(7), e1418. https://doi.org/10.1002/hsr2.1418
6. Sakenova, N., Cacace, E., Orakov, A., Huber, F., Varik, V., Kritikos, G., Michiels, J., Bork, P., Cossart, P., Goemans, C. V., & Typas, A. (2025). Systematic mapping of antibiotic cross-resistance and collateral sensitivity with chemical genetics. *Nature Microbiology*, *10*(1), 202–216. https://doi.org/10.1038/s41564-024-01857-w
7. Barbosa, C., Beardmore, R., Schulenburg, H., & Jansen, G. (2018). Antibiotic combination efficacy (ACE) networks for a Pseudomonas aeruginosa model. *PLOS Biology*, *16*(4), e2004356. https://doi.org/10.1371/journal.pbio.2004356
8. Aulin, L. B. S., Liakopoulos, A., van der Graaf, P. H., Rozen, D. E., & van Hasselt, J. G. C. (2021). Design principles of collateral sensitivity-based dosing strategies. *Nature Communications*, *12*(1), 5691. https://doi.org/10.1038/s41467-021-25927-3
9. Beckley, A. M., & Wright, E. S. (2021). Identification of antibiotic pairs that evade concurrent resistance via a retrospective analysis of antimicrobial susceptibility test results. *The Lancet Microbe*, *2*(10), e545–e554. https://doi.org/10.1016/S2666-5247(21)00118-X
10. Zwep, L. B., Haakman, Y., Duisters, K. L. W., Meulman, J. J., Liakopoulos, A., & van Hasselt, J. G. C. (2021). Identification of antibiotic collateral sensitivity and resistance interactions in population surveillance data. *JAC-antimicrobial resistance*, *3*(4), dlab175. https://doi.org/10.1093/jacamr/dlab175
11. Mahmud, H. A., & Wakeman, C. A. (2024). Navigating collateral sensitivity: Insights into the mechanisms and applications of antibiotic resistance trade-offs. *Frontiers in Microbiology*, *15*, 1478789. https://doi.org/10.3389/fmicb.2024.1478789
12. Pendleton, J. N., Gorman, S. P., & Gilmore, B. F. (2013). Clinical relevance of the ESKAPE pathogens. *Expert Review of Anti-infective Therapy*. https://doi.org/10.1586/eri.13.12

13. Ruekit, S., Srijan, A., Serichantalergs, O., Margulieux, K. R., Mc Gann, P., Mills, E. G., Stribling, W. C., Pimsawat, T., Kormanee, R., Nakornchai, S., Sakdinava, C., Sukhchat, P., Wojnarski, M., Demons, S. T., Crawford, J. M., Lertsethtakarn, P., & Swierczewski, B. E. (2022). Molecular characterization of multidrug-resistant ESKAPEE pathogens from clinical samples in Chonburi, Thailand (2017–2018). *BMC Infectious Diseases*, *22*(1), 695. https://doi.org/10.1186/s12879-022-07678-8
14. Sayers, E. W., Beck, J., Bolton, E. E., Bourexis, D., Brister, J. R., Canese, K., Comeau, D. C., Funk, K., Kim, S., Klimke, W., Marchler-Bauer, A., Landrum, M., Lathrop, S., Lu, Z., Madden, T. L., O'Leary, N., Phan, L., Rangwala, S. H., Schneider, V. A., … Sherry, S. T. (2021). Database resources of the National Center for Biotechnology Information. *Nucleic Acids Research*, *49*(D1), D10–D17. https://doi.org/10.1093/nar/gkaa892
15. Altorf-van der Kuil, W., Schoffelen, A. F., de Greeff, S. C., Thijsen, S. F., Alblas, H. J., Notermans, D. W., Vlek, A. L., van der Sande, M. A., Leenstra, T., & National AMR Surveillance Study Group. (2017). National laboratory-based surveillance system for antimicrobial resistance: A successful tool to support the control of antimicrobial resistance in the Netherlands. *Euro Surveillance*, *22*(46), 17–00062. https://doi.org/10.2807/1560-7917.ES.2017.22.46.17-00062
16. Catalán, P., Wood, E., Blair, J. M. A., Gudelj, I., Iredell, J. R., & Beardmore, R. E. (2022). Seeking patterns of antibiotic resistance in ATLAS, an open, raw MIC database with patient metadata. *Nature Communications*, *13*(1), 2917. https://doi.org/10.1038/s41467-022-30635-7
17. Berends, M. S., Luz, C. F., Friedrich, A. W., Sinha, B. N. M., Albers, C. J., & Glasner, C. (2022). Amr: An R Package for Working with Antimicrobial Resistance Data. *Journal of Statistical Software*, *104*, 1–31. https://doi.org/10.18637/jss.v104.i03
18. Nichol, D., Rutter, J., Bryant, C., Hujer, A. M., Lek, S., Adams, M. D., Jeavons, P., Anderson, A. R. A., Bonomo, R. A., & Scott, J. G. (2019). Antibiotic collateral sensitivity is contingent on the repeatability of evolution. *Nature Communications*, *10*(1), 334. https://doi.org/10.1038/s41467-018-08098-6
19. Hernando-Amado, S., Sanz-García, F., & Martínez, J. L. (2020). Rapid and robust evolution of collateral sensitivity in Pseudomonas aeruginosa antibiotic-resistant mutants. *Science Advances*, *6*(32), eaba5493. https://doi.org/10.1126/sciadv.aba5493
20. Obolski, U., Dellus-Gur, E., Stein, G. Y., & Hadany, L. (2016). Antibiotic cross-resistance in the lab and resistance co-occurrence in the clinic: Discrepancies and implications in E.coli. *Infection, Genetics and Evolution: Journal of Molecular Epidemiology and Evolutionary Genetics in Infectious Diseases*, *40*, 155–161. https://doi.org/10.1016/j.meegid.2016.02.017
21. Allen, R. C., Pfrunder-Cardozo, K. R., & Hall, A. R. (2021). Collateral Sensitivity Interactions between Antibiotics Depend on Local Abiotic Conditions. *mSystems*, *6*(6), e0105521. https://doi.org/10.1128/mSystems.01055-21
22. Imamovic, L., Ellabaan, M. M. H., Machado, A. M. D., Citterio, L., Wulff, T., Molin, S., Johansen, H. K., & Sommer, M. O. A. (2018). Drug-Driven Phenotypic Convergence Supports Rational Treatment Strategies of Chronic Infections. *Cell*, *172*(1), 121–134.e14. https://doi.org/10.1016/j.cell.2017.12.012
23. Liakopoulos, A., Aulin, L. B. S., Buffoni, M., Fragkiskou, E., van Hasselt, J. G. C., & Rozen, D. E. (2022). Allele-specific collateral and fitness effects determine the dynamics of fluoroquinolone resistance evolution. *Proceedings of the National Academy of Sciences of the United States of America*, *119*(18), e2121768119. https://doi.org/10.1073/pnas.2121768119
24. García-Quintanilla, M., Carretero-Ledesma, M., Moreno-Martínez, P., Martín-Peña, R., Pachón, J., & McConnell, M. J. (2015). Lipopolysaccharide loss produces partial colistin dependence and collateral sensitivity to azithromycin, rifampicin and vancomycin in Acinetobacter baumannii. *International Journal of Antimicrobial Agents*, *46*(6), 696–702. https://doi.org/10.1016/j.ijantimicag.2015.07.017
25. Wang, X., Nong, L., Schaar, G., Koenders, B., Jonker, M., de Leeuw, W., & Ter Kuile, B. H. (2025). Collateral sensitivity and cross-resistance in six species of bacteria exposed to six classes of antibiotics. *Microbiology Spectrum*, e0098325. https://doi.org/10.1128/spectrum.00983-25
26. Graf, F. E., Goodman, R. N., Gallichan, S., Forrest, S., Picton-Barlow, E., Fraser, A. J., Phan, M.-D., Mphasa, M., Hubbard, A. T. M., Musicha, P., Schembri, M. A., Roberts, A. P., Edwards, T., Lewis, J. M., & Feasey, N. A. (2024). Molecular mechanisms of re-emerging chloramphenicol susceptibility in extended-spectrum beta-lactamase-producing Enterobacterales. *Nature Communications*, *15*(1), 9019. https://doi.org/10.1038/s41467-024-53391-2
27. Pál, C., Papp, B., & Lázár, V. (2015). Collateral sensitivity of antibiotic-resistant microbes. *Trends in Microbiology*, *23*(7), 401–407. https://doi.org/10.1016/j.tim.2015.02.009
28. Rosenkilde, C. E. H., Munck, C., Porse, A., Linkevicius, M., Andersson, D. I., & Sommer, M. O. A. (2019). Collateral sensitivity constrains resistance evolution of the CTX-M-15 β-lactamase. *Nature Communications*, *10*(1), 618. https://doi.org/10.1038/s41467-019-08529-y

Supplementary Figures

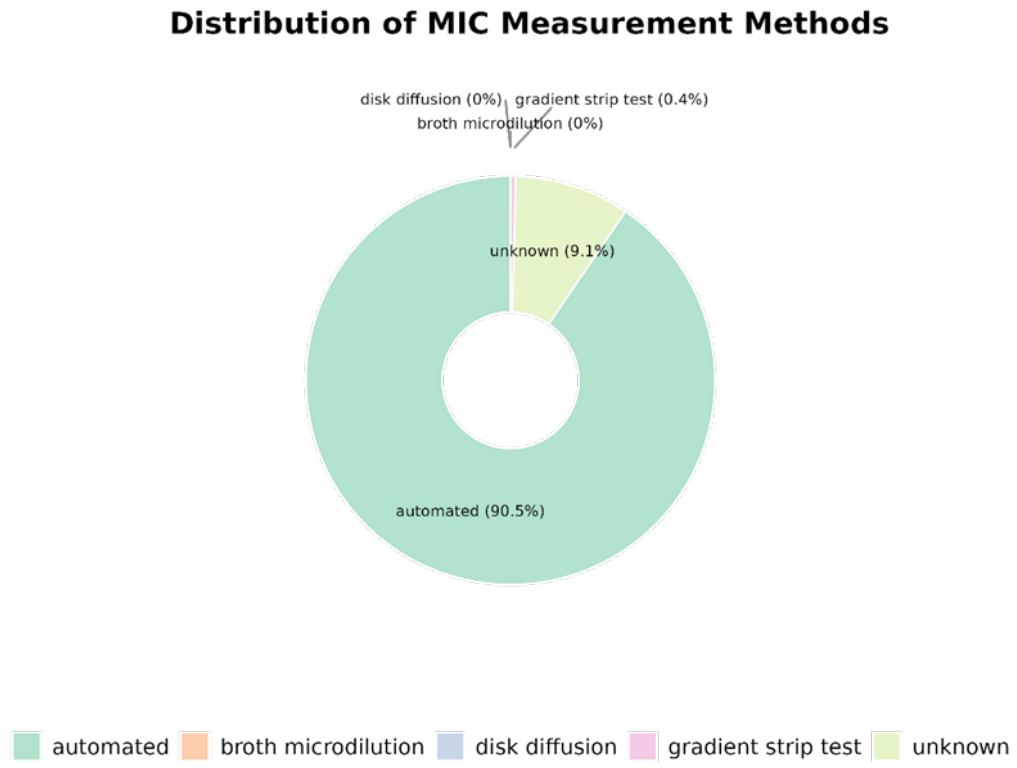

Fig. S1 | MIC measurement method distribution in the pooled dataset. MIC measurements from broth microdilution and disk diffusion consists of less than 0.01% of measurements in the pooled dataset.

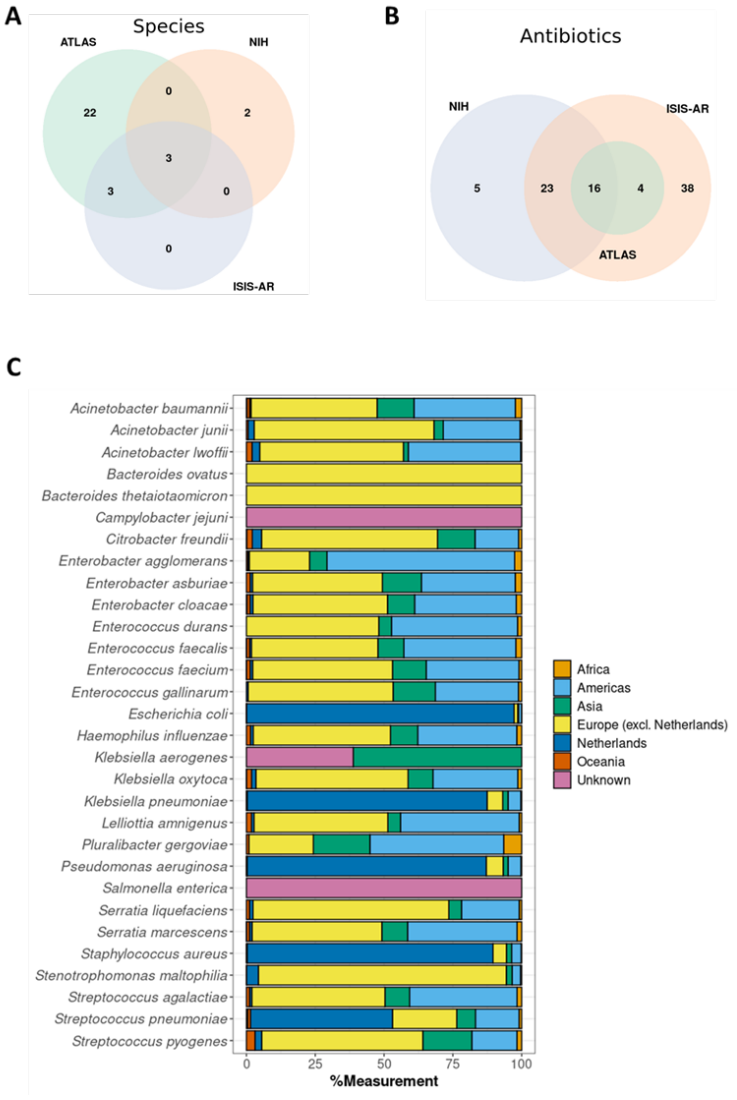

Fig. S2 | Species and antibiotics distribution across the three databases. Venn diagrams showing the A) species distribution and B) antibiotics distribution across the NIH, ISIS-AR, and ATLAS databases. C) Regional distribution of measurement source per species. Netherlands was separated from the rest of Europe to highlight the overwhelming impact of the inclusion of ISIS-AR dataset on *A. baumannii, E. coli, K. pneumoniae, P. aeruginosa, S. aureus, and S. pneumoniae.*

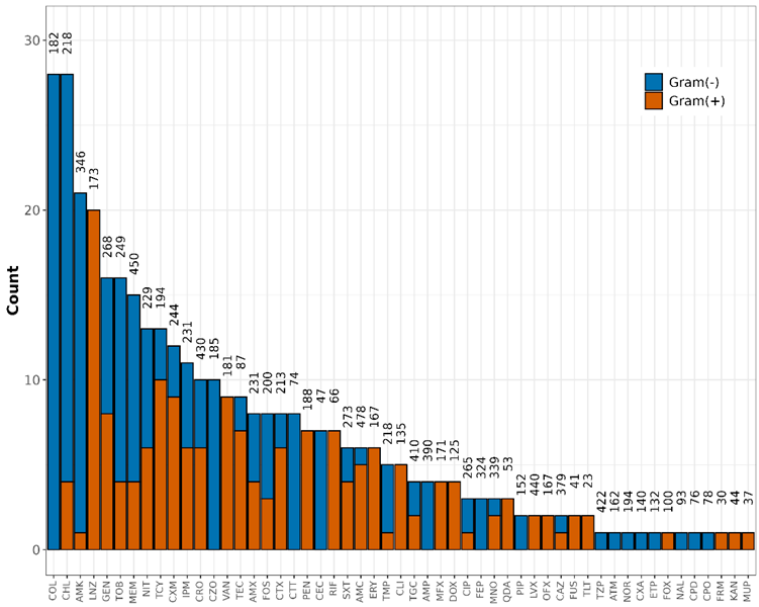

Fig. S3 | CS occurrence in Gram-negative and Gram-positive pathogens. Number of CS pairs identified for each antibiotic stratified by Gram staining classification. The total number of species-antibiotic pairs tested for the antibiotic of interest (including no collateral effects and CR) were shown above the bars. Antibiotics with no identified CS interaction were excluded. Antibiotics name abbreviations are listed in Table S1.

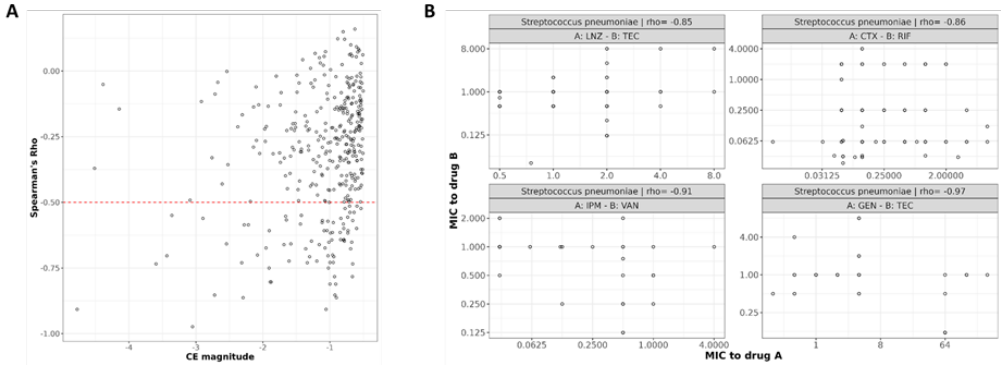

Fig. S4 | Collateral effect magnitude and correlation between MIC to focal and test antibiotics. Inverse proportionality was tested by Spearman's rank correlation. Only antibiotic pairs showing CS were evaluated. A) No strong association was found between Spearman's correlation coefficient (ρ) and the magnitude of the collateral effect (CE). The red dashed line indicates the threshold below which correlations between the MICs of antibiotic pairs are considered strong ($\rho <$ -0.5). Each data point represents the ρ and CE magnitude for a tested antibiotic pair. B) Antibiotic pairs with strongly negative MIC correlations ($\rho <$ -0.85). Only four antibiotic pairs met this threshold. The species in which each pair was tested and the corresponding ρ value are indicated in the top facet label. Drug names for each pair (A and B) are shown in the bottom facet label as "A: [drug A] - B: [drug B]." Each data point represents a strain's MIC values for the two antibiotics in the pair. All four highly correlated CS pairs were identified in *S. pneumoniae*: linezolid (LNZ)-teicoplanin (TEC), cefotaxime (CTX)-rifampicin (RIF), imipenem (IPM)-vancomycin (VAN), and gentamicin (GEN)-TEC. Reciprocal CS was observed for LNZ-TEC, CTX-RIF, and IPM-VAN. Reciprocal CS could not be confirmed for GEN-TEC due to limited variation in GEN MIC among isolates with TEC MICs below the species median (0.12 mg/L).

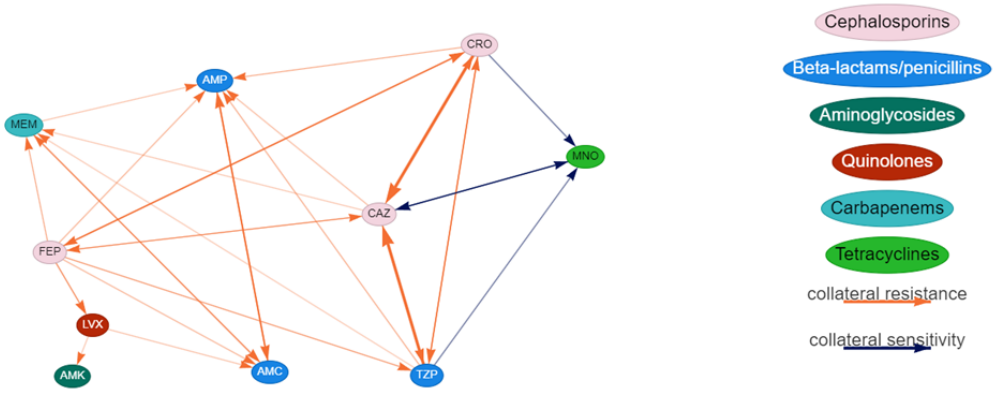

Fig. S5 | Collateral sensitivity network of *Haemophilus influenzae*. The sample network diagram represents the collateral sensitivity network observed in *H. influenzae* with a minimum collateral effect magnitude (ϕ) of 0.5. Arrows denote the CS effect and direction, while the colors denote the different antibiotic classes. Further exploration of the collateral effect network is accessible at collateralviz.lacdr.leidenuniv.nl.

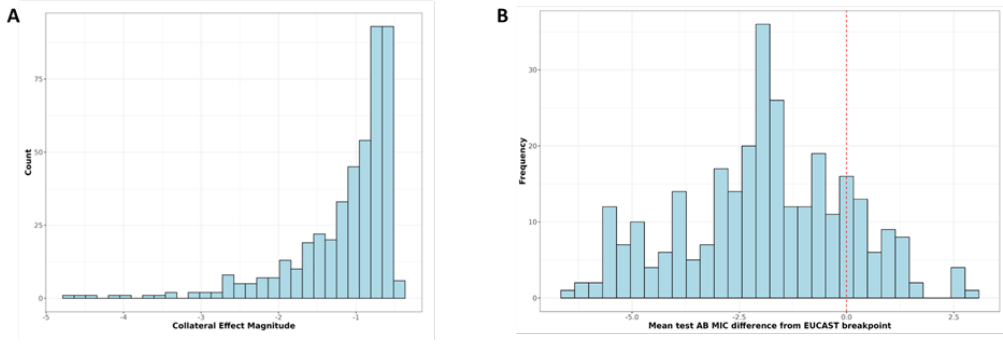

Fig. S6 | Magnitude of CS effect on test antibiotic MIC. A) Distribution of collateral effect magnitudes for all identified CS interactions. B) log2-difference in the MIC of test antibiotics for pathogens with higher MIC to the focal antibiotic, relative to the corresponding EUCAST or CLSI MIC breakpoint (indicated by the red dashed line). Mean log2-MIC difference from breakpoint is 1.89 across all identified CS pairs where MIC breakpoint value for the test antibiotics was available. MIC breakpoint value was obtained from the 'AMR' package in R.

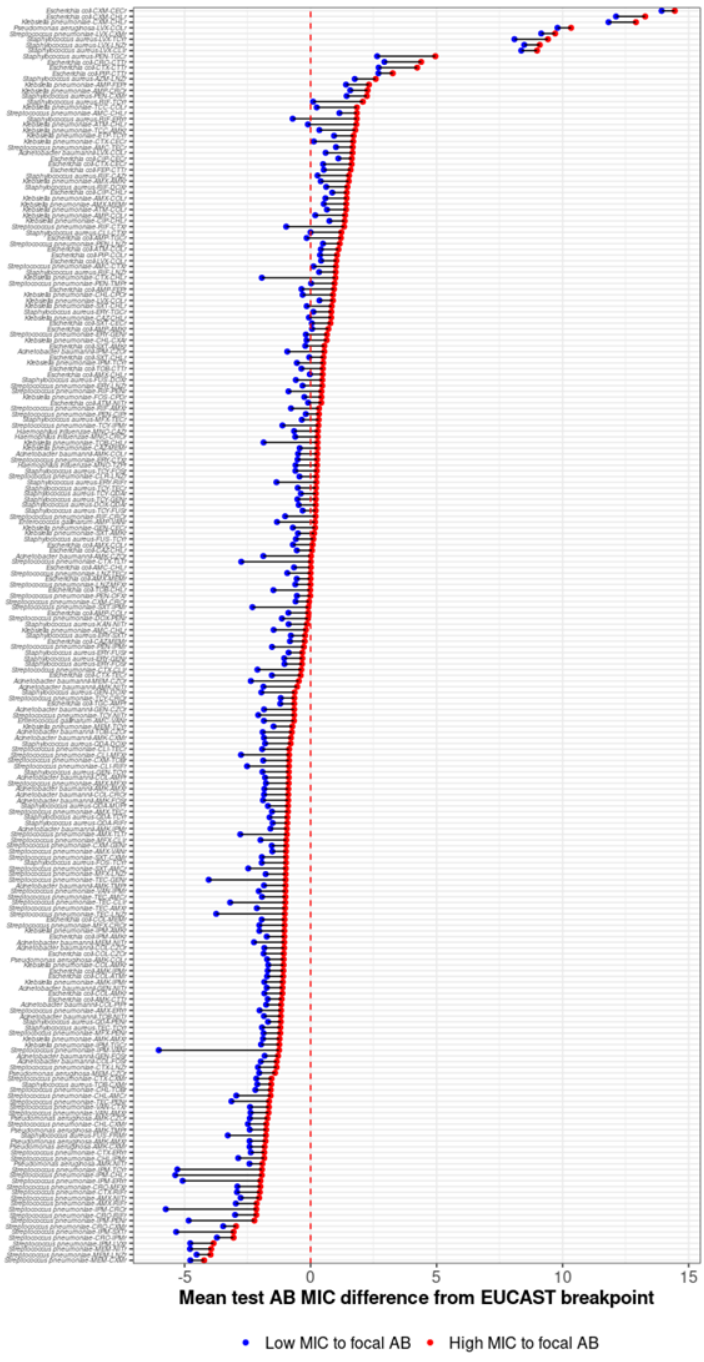

Fig. S7 | MIC difference of test antibiotics relative to the corresponding clinical breakpoint. Mean log2-MIC differences from the MIC breakpoint for test antibiotics are shown for isolates with lower (red dots) and higher (blue dots) MICs to the focal antibiotic. Line segments connect each pair of MIC values included in a collateral effect test. The red dashed line indicates zero difference; line segments crossing this line indicated CS interactions where the mean test antibiotic MIC shifted from above to below the susceptibility breakpoint (observed in 14.2% of CS pairs with known breakpoint value). Only CS interactions are shown. Species-test antibiotic combinations without available EUCAST/CLSI MIC breakpoints were excluded (18.7% of all identified CS interactions). MIC breakpoint value was obtained from the 'AMR' package in R.

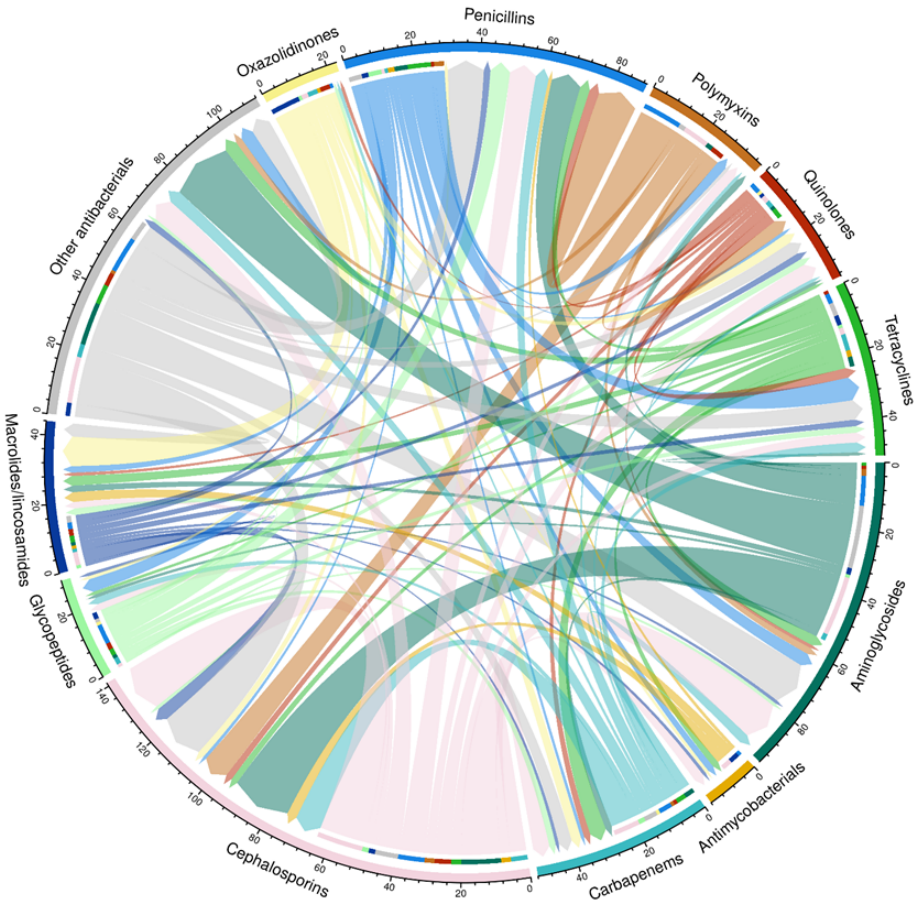

Fig. S8 | Prevalence and direction of intra-class CS. Arrows (chords) originate from the focal antibiotic class (where higher MIC was observed) and point toward the test antibiotic class (where CS effects were detected). The color of the inner arc at the base of each arrow corresponds to the antibiotic class of the test antibiotic (the class at which the arrow ends), while the color of the outer arc represents the antibiotic class at each segment of the circle. The color of each chord matches the color of the test antibiotic class, providing a consistent visual link between the arc and its associated interactions. The width of each arrow chord is proportional to the number of detected CS interactions between the focal and test classes. Numbers at the outer arcs indicate the total number of detected CS interactions either originating from (start) or received by (end) each antibiotic class. The 'Other antibacterials' class includes chloramphenicol, daptomycin, fosfomycin, fusidic acid, metronidazole, mupirocin, nitrofurantoin, sulfamethoxazole, sulfisoxazole, trimethoprim, trimethoprim/sulfamethoxazole, and zidebactam. The β-lactam class was here separated into penicillins, cephalosporins, and carbapenems. No observed CS involved monobactams.

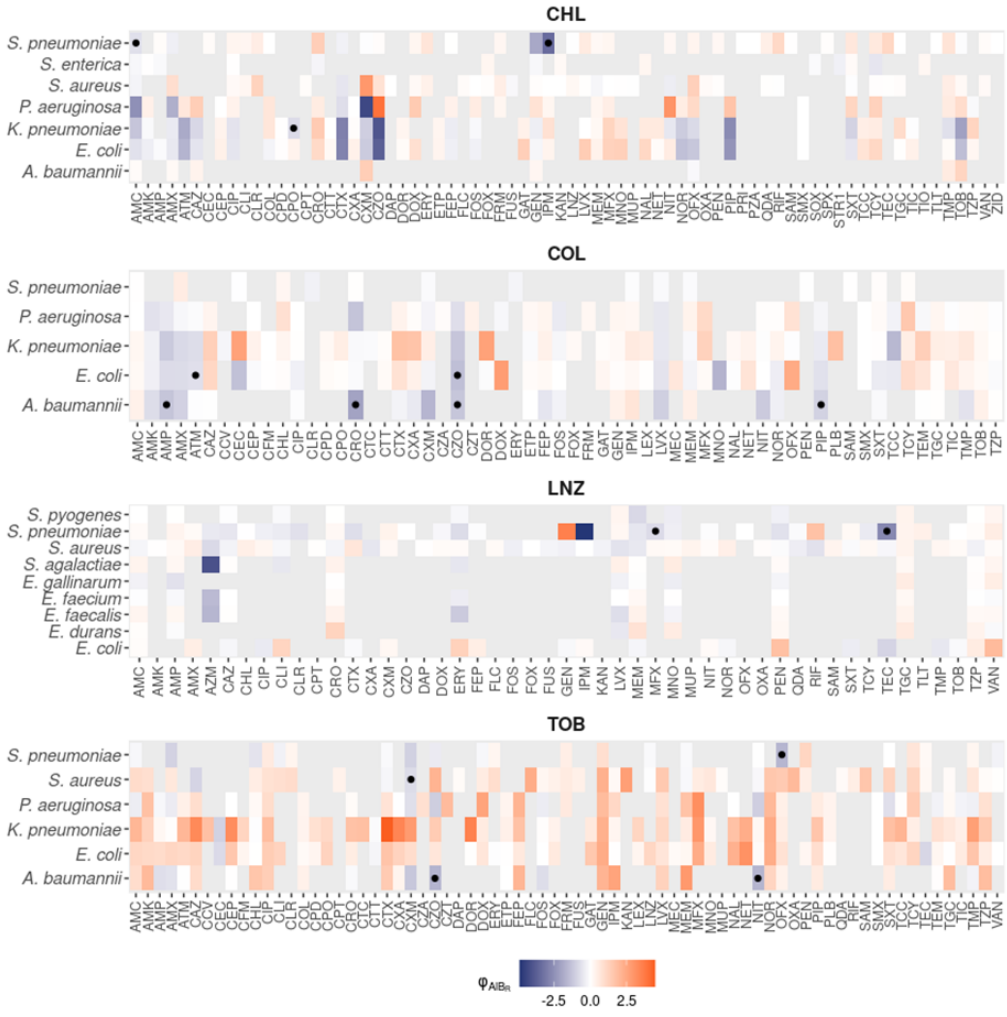

Fig. S9 | Collateral effect distribution across species in strains with a high MIC to CHL, COL, LNZ, and TOB. Collateral effect magnitude ϕ is shown as color on each drug combination-species set. The absence of collateral effect is denoted by the color white. CS and CR are denoted by blue and red color gradient, respectively. Drug combination-species sets where data was incomplete/missing are shown as grey tiles. Reciprocal CS are marked by dots. Collateral effect distributions in pathogens resistant to other drugs are available in the supplementary data.

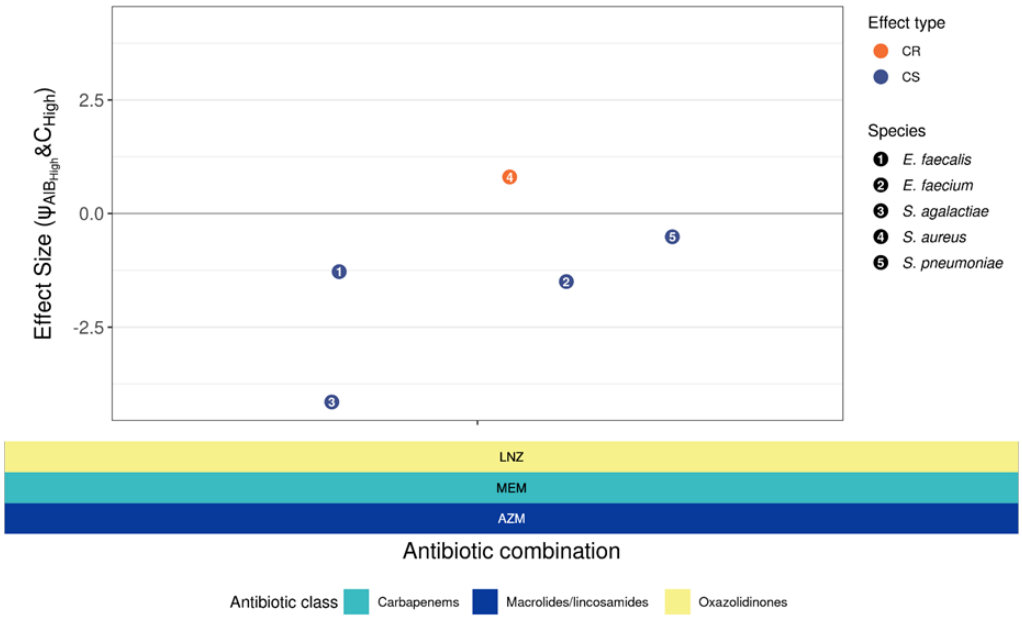

Fig. S10 | Magnitude and species distribution of AZM sensitivity in isolates with high MIC to LNZ and MEM. CS interactions were considered consistent if the effect was observed in at least 4 different species. The magnitude of the three-way collateral effect was expressed by ψ (Eq. 2). Drug label colors denoted the different antibiotic classes between which the CS effect was detected. The number of species shown for each three-antibiotic pair may vary based on data availability, as species with fewer than 100 MIC measurements for a given triplet were excluded from the analysis. Antibiotic name abbreviations are listed in Table S1.

Supplementary Tables

Table S1. Antibiotics class and 3-letter code

Antibiotics	Class	3-letter code
amoxicillin/clavulanic acid	Beta-lactams/penicillins	AMC
amikacin	Aminoglycosides	AMK
ampicillin	Beta-lactams/penicillins	AMP
amoxicillin	Beta-lactams/penicillins	AMX
aztreonam	Beta-lactams/penicillins	ATM
azithromycin	Macrolides/lincosamides	AZM
ceftazidime	Cephalosporins (3rd gen.)	CAZ
ceftazidime/clavulanic acid	Cephalosporins (3rd gen.)	CCV
cefaclor	Cephalosporins (2nd gen.)	CEC
cefalotin	Cephalosporins (1st gen.)	CEP
cefixime	Cephalosporins (3rd gen.)	CFM
chloramphenicol	Amphenicols	CHL
ciprofloxacin	Quinolones	CIP
clindamycin	Macrolides/lincosamides	CLI
clarithromycin	Macrolides/lincosamides	CLR
colistin	Polymyxins	COL
cefpodoxime	Cephalosporins (3rd gen.)	CPD
cefpirome	Cephalosporins (4th gen.)	CPO
ceftaroline	Cephalosporins (5th gen.)	CPT
ceftriaxone	Cephalosporins (3rd gen.)	CRO
cefotaxime/clavulanic acid	Cephalosporins (3rd gen.)	CTC
cefotetan	Cephalosporins (2nd gen.)	CTT
cefotaxime	Cephalosporins (3rd gen.)	CTX
cefuroxime axetil	Cephalosporins (2nd gen.)	CXA
cefuroxime	Cephalosporins (2nd gen.)	CXM
ceftazidime/avibactam	Cephalosporins (3rd gen.)	CZA
cefazolin	Cephalosporins (1st gen.)	CZO
ceftolozane/tazobactam	Cephalosporins (5th gen.)	CZT
daptomycin	Other antibacterials	DAP
doripenem	Carbapenems	DOR
doxycycline	Tetracyclines	DOX
erythromycin	Macrolides/lincosamides	ERY
ertapenem	Carbapenems	ETP
cefepime	Cephalosporins (4th gen.)	FEP
flucloxacillin	Beta-lactams/penicillins	FLC
fosfomycin	Other antibacterials	FOS
cefoxitin	Cephalosporins (2nd gen.)	FOX
framycetin	Aminoglycosides	FRM
fusidic acid	Other antibacterials	FUS
gatifloxacin	Quinolones	GAT
gentamicin	Aminoglycosides	GEN
imipenem	Carbapenems	IPM
kanamycin	Aminoglycosides	KAN
cefalexin	Cephalosporins (1st gen.)	LEX
linezolid	Oxazolidinones	LNZ
levofloxacin	Quinolones	LVX
mecillinam	Beta-lactams/penicillins	MEC
meropenem	Carbapenems	MEM
moxifloxacin	Quinolones	MFX

Based on the 'AMR' package.

Table S1. Antibiotics class and 3-letter code (continued)

Antibiotics	Class	3-letter code
minocycline	Tetracyclines	MNO
metronidazole	Other antibacterials	MTR
mupirocin	Other antibacterials	MUP
nalidixic acid	Quinolones	NAL
netilmicin	Aminoglycosides	NET
nitrofurantoin	Other antibacterials	NIT
norfloxacin	Quinolones	NOR
ofloxacin	Quinolones	OFX
oxacillin	Beta-lactams/penicillins	OXA
benzylpenicillin	Beta-lactams/penicillins	PEN
piperacillin	Beta-lactams/penicillins	PIP
polymyxin B	Polymyxins	PLB
pristinamycin	Macrolides/lincosamides	PRI
pyrazinamide	Antimycobacterials	PZA
quinupristin/dalfopristin	Macrolides/lincosamides	QDA
rifampicin	Antimycobacterials	RIF
ampicillin/sulbactam	Beta-lactams/penicillins	SAM
sulfamethoxazole	Trimethoprims	SMX
sulfisoxazole	Other antibacterials	SOX
sparfloxacin	Quinolones	SPX
streptomycin	Aminoglycosides	STR1
trimethoprim/sulfamethoxazole	Trimethoprims	SXT
ticarcillin/clavulanic acid	Beta-lactams/penicillins	TCC
tetracycline	Tetracyclines	TCY
teicoplanin	Glycopeptides	TEC
temocillin	Beta-lactams/penicillins	TEM
tigecycline	Tetracyclines	TGC
ticarcillin	Beta-lactams/penicillins	TIC
ceftiofur	Cephalosporins (3rd gen.)	TIO
telithromycin	Macrolides/lincosamides	TLT
trimethoprim	Trimethoprims	TMP
tobramycin	Aminoglycosides	TOB
piperacillin/tazobactam	Beta-lactams/penicillins	TZP
vancomycin	Glycopeptides	VAN
zidebactam	Other antibacterials	ZID

Based on the 'AMR' package.

Table S2. Reciprocal pairwise CS pairs involving COL or CHL.

Antibiotics		**CS magnitude (focal → test)**		$\mathbf{n_{measurements}}$	**Species**
A	**B**	**A → B**	**B → A**		
COL	PIP	-0.59	-1.00	1482	*A. baumannii*
COL	CRO	-0.96	-2.08	1627	*A. baumannii*
COL	CZO	-0.78	-1.27	837	*A. baumannii*
COL	AMP	-0.94	-1.30	290	*A. baumannii*
COL	ATM	-0.64	-0.70	77739	*E. coli*
COL	CZO	-0.80	-1.44	35057	*E. coli*
CHL	CPO	-1.20	-0.79	247	*K. pneumoniae*
CHL	AMC	-1.36	-0.69	2772	*S. pneumoniae*
CHL	IPM	-1.03	-3.43	1726	*S. pneumoniae*